On the barium - oxygen consumption relationship in the Mediterranean Sea: implications for mesopelagic marine snow remineralisation.

Stéphanie H.M. Jacquet[1*], Dominique Lefèvre[1], Christian Tamburini[1], Marc Garel[1], Frédéric A.C. Le Moigne[1], Nagib Bhairy[1], Sophie Guasco[1]

[1]Aix Marseille Université, CNRS/INSU, Université de Toulon, IRD, Mediterranean Institute of Oceanography (MIO), UM 110, 13288 Marseille, France,

[*]Correspondence to: S. Jacquet (*stephanie.jacquet@mio.osupytheas.fr)*

Biogeosciences

ABSTRACT

In the ocean, remineralisation rate associated with sinking particles is a crucial variable. Since the 90's, particulate biogenic barium (Ba_{xs}) has been used as an indicator of carbon remineralization by applying a transfer function relating Ba_{xs} to O_2 consumption (Dehairs's transfer function, Southern Ocean-based). Here, we tested its validity in the Mediterranean Sea (ANTARES / EMSO-LO) for the first time by investigating connections between Ba_{xs}, prokaryotic heterotrophic production (PHP) and oxygen consumption (JO_2-Opt; optodes measurement). We show that: (1) higher Ba_{xs} (409 pM; 100- 500 m) occurs in situations where integrated PHP (PHP100/500= 0.90) is located deeper, (2) higher Ba_{xs} occurs with increasing JO_2-Opt, and (3) similar magnitude between JO_2-Opt (3.14 mmol m^{-2} d^{-1}; 175- 450 m) and JO_2-Ba (4.59 mmol m^{-2} d^{-1}; transfer function). Overall, Ba_{xs}, PHP and JO_2 relationships follow trends observed earlier in the Southern Ocean. We conclude that such transfer function could apply in the Mediterranean Sea.

KEY WORDS: particulate biogenic barium, mesopelagic zone, oxygen consumption, prokaryotic heterotrophic production, carbon remineralization, Mediterranean Sea

1. INTRODUCTION

Ocean ecosystems play a critical role in the Earth's carbon (C) cycle [IPCC, 2014]. The quantification of their impacts of both present conditions and future predictions remains one of the greatest challenges in oceanography [Siegel et al., 2016]. In essence, the biological C pump is termed for the numerous processes involved in maintaining the vertical gradient in dissolved inorganic C. This includes processes such as organic matter production in surface, its export and subsequent remineralization. Most of marine snow organic C conversion (i.e. remineralization) into CO_2 by heterotrophic organisms (i.e. respiration) occurs in the mesopelagic zone (100-1000 m) [Martin et al., 1987; Buesseler and Boyd, 2009]. Globally, the flux of C exported below 1000 m depth is the key determinant of ocean carbon storage capacity [Henson et al., 2011]. However, there is no consensus on C transfer efficiency estimations from field experiments, leading to an imbalance of the water column C budget [Giering et al., 2014]. Resolving this imbalance is in the core of numerous studies in the global ocean, but also regionally, especially in the Mediterranean Sea (MedSea). Due to limited exchanges with adjacent basin and the existence of an intense overturning circulation qualitatively resembling the global one (but with shorter time scales), the MedSea is often considered as a laboratory to observe and understand the impact of transient climate variability on ecosystems and biogeochemical cycles [Malanotte-Rissoli et al., 2014]. In a context of climate changes, better constraining C fluxes and the ocean C storage capacity is of crucial importance.

Particulate barium in excess (Ba_{xs}, i.e. biogenic Ba from total particulate Ba after correction for lithogenic Ba) is a geochemical tracer of particulate organic carbon (POC) remineralization in the mesopelagic layer [Dehairs et al., 1997]. Ba_{xs} mostly occurs in the form of barite microcrystals ($BaSO_4$) at these depths. In a global ocean undersaturated with respect to barite, studies report that Ba_{xs} would precipitate inside oversaturated biogenic micro-environments during POC

60 degradation by heterotrophic prokaryotes in the mesopelagic zone, through sulfate and/or barium
61 enrichment [Bertram and Cowen, 1997]. The first-ever studies on mesopelagic Ba_{xs} reported
62 coinciding Ba_{xs} maxima with depths of dissolved O_2 minimum and pCO_2 maximum [Dehairs et
63 al., 1987, 1997]. By using an 1D advection-diffusion model applied to O_2 profiles in the Atlantic
64 sector of the Southern Ocean (ANTX/6 cruise; Shopova et al., 1995), Dehairs et al. [1997]
65 established an algorithm converting mesopelagic Ba_{xs} concentration into O_2 consumption rate
66 (JO_2) and organic C remineralized (POC remineralization rate). This transfer function has been
67 widely used until now [Cardinal et al., 2001, 2005; Dehairs et al., 2008; Jacquet et al., 2008a,
68 2008b, 2011, 2015]. Yet its validity has never been tested in other oceanic provinces. In the
69 North Atlantic, Lemaitre et al. [2018] reported a Ba_{xs} - JO_2 (obtained from apparent oxygen
70 utilisation divided by the water mass age) relationship not significantly different to that reported
71 in Dehairs et al. [1997]. Furthermore, significant progresses were made in relating Ba_{xs}, O_2
72 dynamics to prokaryotic heterotrophic activity [Jacquet et al., 2015]. These advancements clearly
73 show that Ba_{xs} is closely related with the vertical distribution of prokaryotes heterotrophic
74 production (PHP) (the rate of change with depth), reflecting the temporal progression of POC
75 remineralization processes. Also, in a first attempt to test the validity of the Dehairs's transfer
76 function in other locations, Jacquet et al. [2015] confronted oxygen consumption rates (JO_2) from
77 direct measurements (dark community respiration, DCR) to derived JO_2 from Ba_{xs} data (using the
78 transfer function) in the Kerguelen area (Indian sector of the Southern Ocean). We revealed good
79 convergence of JO_2 rates from these two approaches, further supporting the Dehairs's function to
80 estimate POC remineralization rates in different biogeochemical settings of the Southern Ocean.
81 Here, we further investigate relationships between the mesopelagic Ba_{xs} proxy, prokaryotic
82 activity and oxygen dynamics (Figure 1a) in the northwestern Mediterreanean Sea (MedSea), a
83 different biogeochemical setting to those already studied (see references above). Today,

observations of the various components of the MedSea biological C pump provide organic C remineralization fluxes varying by at least an order of magnitude [Santinelli et al., 2010; Ramondenc et al., 2016]. Malanotte-Rissoli et al. [2014] reviewing unsolved issues and future directions for MedSea research highlighted the need to further investigate biogeochemical processes at intermediate (mesopelagic) and deep layers to reconciliate the C budget in the Mediterranean basin. Previous particulate Ba_{xs} dataset is very scarce in the NW- MedSea, with in general very low vertical sampling resolution [Sanchez Vidal et al., 2005] or very restricted studied areas [Dehairs et al., 1987; Sternberg et al., 2008]. Here we discuss Ba_{xs}, PHP and JO_2 (from optodes measurement during incubations) at the ANTARES / EMSO-LO observatory site (Figure 1a, b). We hypothesize that the Dehairs's transfer function converting Ba_{xs} into POC remineralization also applies in a different ocean ecosystem functioning from the Southern Ocean. We suggest that the Ba_{xs} proxy can be used as routine tracer to estimate local-scale processes of mesopelagic POC remineralization in the Mediterranean basin.

2. METHODS

2.1 STUDY SITE

The BATMAN cruise (https://doi.org/10.17600/16011100, March 10-16 2016, *R/V* EUROPE) took place to the ANTARES / EMSO-LO observatory site (42°48'N, 6°10'E; Tamburini et al., 2013), 40 km off the coast of Toulon, southern France (Figure 1b). The hydrological and biogeochemical conditions at this site are monitored monthly in the framework of the MOOSE (Mediterranean Ocean Observing System for the Environment) program and of the EMSO (European Multidisciplinary Subsea Observatory) observation program. The hydrography displays the general three-layer MedSea system with surface, intermediate and deep waters [Hainbucher et al., 2014]. Briefly, the main water masses can be distinguished (see potential

temperature – salinity diagram during the BATMAN cruise in Figure 1c): (1) Surface Water (SW); (2) Winter Intermediate Water (WIW); (3) Levantine Intermediate water (LIW). LIW is present at intermediate depths (around 400 m at ANTARES) and is characterized by temperature and a salinity maxima; (4) Mediterranean Deep Water (MDW).

2.2 SAMPLING AND ANALYSES

For particulate barium, 4 to 7 L of seawater sampled using Niskin bottles were filtered onto 47 mm polycarbonate membranes (0.4 μm porosity) under slight overpressure supplied by filtered air. Filters were rinsed with few mL of Milli-Q grade water to remove sea salt, dried (50°C) and stored in Petri dishes. Thirteen depths between surface and 1000 m were sampled by combining different casts sampled closely in time and space (total of 28 samples) with similar potential temperature – salinity profiles. No major changes in water mass characteristics occured over the 3-day sampling period (Figure 1c). In the laboratory, we performed a total digestion of filters using a concentrated tri-acid (0.5 mL HF /1.5 mL HNO_3 / HCl 1 mL; all Optima grade) mixture in closed teflon beakers overnight at 95°C in a clean pressurized room. After evaporation close to dryness, samples were re-dissolved into 10 mL of HNO_3 2%. The solutions were analysed for Ba and other elements of interest (Na and Al) by HR-ICP-MS (High Resolution-Inductively Coupled Plasma- Mass Spectrometry; ELEMENT XR ThermoFisher). Based on analyses of external certified reference standards, accuracy and reproducibility were both within ±5%. Details on sample processing and analysis are given in Cardinal et al. [2001] and Jacquet et al. [2015]. The presence of sea-salt was checked by analysing Na and the sea-salt particulate Ba contribution was found negligible (<0.1% of total Ba). Particulate biogenic barium in excess (hereafter referred to as Ba_{xs}) was calculated as the difference between total Ba and lithogenic Ba using Al as the lithogenic reference element. The lithogenic Ba concentration was determined using Al

concentration and the upper continental crust (UCC) Ba:Al molar ratio [Taylor and Mc.Lennan, 1985]. The biogenic Ba fraction ranged from 51 to 91 % of the total particulate Ba signal (see section 3.1). The standard uncertainty [Ellison et al., 2000] on Ba_{xs} concentration ranges between 5.0 and 5.5%. The term "in excess" is used to indicate that concentrations are larger than the Ba_{xs} background. The background (or residual value) is considered as "preformed" Ba_{xs} at zero oxygen consumption left over after transfer and partial dissolution of Ba_{xs} produced during degradation of previous phytoplankton growth events. The background is set at 130 pM in this study.

Oxygen concentrations were measured using oxygen optode Aanderaa® 4330 for at least 24 hours (on a 30 seconds time step) on samples taken at 4 depths in the mesopelagic layer (175, 250, 450 and 1000 m). Samples were placed into a sealed 1L borosilicate glass bottles incubated at a constant temperature of 13°C in thermo-regulated baths. Optodes were calibrated using a home made calibration facility (https://www.mio.osupytheas.fr/en/cybele/oxygen-dynamics-construction-oxygen-optode-calibration-platform). Oxygen consumption rates (later referred to as JO_2-Opt) were derived from a linear model calculation. Associated errors to the linear model fit are below 0.01 µM O_2 h^{-1}. Each oxygen consumption experiment has been duplicated for each depth. Average and standard deviation of the duplicates are reported in Fig 3a. The larger associated errors are related to the differences between each duplicates, especially in surface, reflecting potential heterogeneity of the microbial community during sampling.

Prokaryotic heterotrophic production (PHP) estimation was measured over time course experiments at *in situ* temperature (13°C) following the protocol described in Tamburini et al. [2002]. ^{3}H-leucine labelled tracer [Kirchman, 1993] was used. To calculate prokaryotic heterotrophic production, we used the empirical conversion factor of 1.55 ng C per pmol of

incorporated leucine according to Simon and Azam [1989], assuming that isotope dilution was negligible under these saturating concentrations.

3. RESULTS AND DISCUSSION

3.1 Particulate Ba_{xs} vertical distribution

Particulate biogenic Ba_{xs}, particulate Al (pAl) and biogenic Ba fraction profiles in the upper 1000 m at ANTARES are reported in Figure 2a. Ba_{xs} concentrations range from 12 to 719 pM. The biogenic Ba fraction ranges from 51 to 91 % of the total particulate Ba signal. Particulate Al concentrations (pAl) range from 8 to 170 nM. Ba_{xs} concentrations are low in surface water (<100 pM) where the lithogenic fraction reaches 43 to 49 % in the upper 70 m. From previous studies we know that Ba_{xs} in surface waters is distributed over different, mainly non-barite biogenic phases, and incorporated into or adsorbed onto phytoplankton material. As such these do not reflect POC remineralization processes, in contrast to mesopelagic waters where Ba_{xs} is mainly composed of barite formed during prokaryotic degradation of organic matter. Focus is done in the present study on the mesopelagic layer. The Ba_{xs} profile at ANTARES indeed displays a mesopelagic Ba_{xs} maximum between 100 and 500 m, reaching up to 719 pM at 175 m. Ba is mostly biogenic at these depths (> 80 %). Ba_{xs} concentrations then decrease below 500 m to reach a background value of around 130 pM (see BKG in Figure 2). Note that the MedSea is largely undersaturated with respect to barite, with saturation state ranging between 0.2 and 0.6 over the basin [Jacquet et al., 2016; Jullion et al., 2017]. For comparison, the Ba_{xs} background value in the Southern Ocean reaches 180 to 200 pM below 1000 m [Dehairs et al., 1997; Jacquet et al. 2015]. Previously, Sternberg et al. [2008] reported the seasonal evolution of Ba_{xs} profiles at the DYFAMED station (43°25'N-7°52'E; BARMED project) northeast from ANTARES (Figure 1c) in the NW-MedSea. The present Ba_{xs} profile at ANTARES (March 2016) is very similar to

179 the Ba_{xs} profile measured in March 2003 at DYFAMED (Figure 2a). The slight difference
180 between Ba_{xs} profiles in the upper 75 m suggests more Ba bounded and/or adsorbed onto
181 phytoplankton material during BARMED. Both profiles present a Ba_{xs} maximum in the upper
182 mesopelagic zone between 150 and 200 m. Below this maximum, Ba_{xs} concentrations gradually
183 decrease to reach around 130 pM between 500 and 1000 m (this study). A similar value was
184 reached between 500 and 600 m at the DYFAMED station over the whole studied period
185 (between February and June 2003; Sternberg et al., 2008).
186
187 **3.2 Prokaryotic heterotrophic production**
188 The particulate Ba in excess is centred in the upper mesopelagic zone between 100 and 500 m
189 and reflects that POC remineralization mainly occurred at this depth layer (Figure 2a). Depth-
190 weighted average (DWA) Ba_{xs} content (409 pM), i.e. the Ba_{xs} inventory divided by the depth
191 layer considered, was calculated between 100 and 500 m. Figure 2b shows the column-integrated
192 PHP at 100 m over the one at 500 m (PHP100/500). Our PHP100/500 ratio at ANTARES station
193 is of 0.90 and is compared to results obtained during KEOPS1 (summer) and KEOPS2 (spring;
194 out plateau stations) cruises in the Southern Ocean [Jacquet et al., 2008; 2015] and #DY032
195 cruise (July 2015, *R/V* DISCOVERY) at the PAP (Porcupine Abyssal Plain) observatory in the
196 northeast Atlantic (49°N, 16.5 °W) (personal data). Result at the ANTARES / EMSO-LO site
197 follows the trend previously reported in the Southern Ocean (blue line in Figure 2b; Jacquet et al.,
198 2015), indicating higher DWA Ba_{xs} in situations where a significant part of column-integrated
199 PHP is located deeper in the water column (high Int. PHPx1/IntPHPx2 ratio; Figure 2b). These
200 previous studies revealed that the shape of the column-integrated PHP profile (i.e. the attenuation
201 gradient) is important in setting the Ba_{xs} signal in the mesopelagic zone (Dehairs et al., 2008;
202 Jacquet et al., 2008, 2015]. Indeed, mesopelagic DWA Ba_{xs} appears reduced when most of the

column-integrated PHP is limited to the upper layer, i.e. indicating an efficient remineralization in surface. In contrast, mesopelagic DWA Ba_{xs} appears higher when most of the column-integrated PHP is located in the mesopelagic layer, i.e. reflecting significant deep PHP activity, POC export and subsequent remineralization (Figure 2b). Results at the PAP site reflect a similar situation as observed during KEOPS2 for time series stations at Plateau site and in a meander of the polar front area (not show in Figure 2b). At these stations, Jacquet et al. [2015] reported a shift toward the KEOPS1 trend reflecting the temporal evolution (season advancement) and patchiness of the establishment of mesopelagic remineralization processes within a same area. Overall, our MedSea result is located along the trend defined in the Southern Ocean during KEOPS1 cruise. It is generally considered that Ba_{xs} (barite) forms inside sulfate and/or barium oversaturated biogenic micro-environments during POC degradation by heterotrophic prokaryotes. However, it is unclear whether barite formation at mesopelagic depths is (directly or indirectly) bacterially induced or bacterially influenced [Martinez-Ruiz et al., 2018, 2019]. In any case our results strengthen the close link between the water column Ba_{xs} distribution and respiration (organic matter degradation).

3.3 Oxygen- barium relationship

The relationship we obtained at ANTARES between Ba_{xs} concentrations and oxygen consumption rates from optodes measurements (JO_2-Opt) is reported in Figure 3a. JO_2-Opt range from 0.11 to 5.85 μmol L^{-1} d^{-1}. The relationship indicates higher Ba_{xs} concentrations with increasing JO_2-Opt. An interesting feature is the intercept at zero JO_2-Opt (around 128 pM) which further supports the Ba BKG value at ANTARES (130 pM) determined from measured Ba_{xs} profiles (Figure 3a).

In figure 3b we applied a similar approach as reported in Jacquet et al. [2015] where we show the correlation between JO_2 obtained from dark community respiration DCR (Winkler titration; JO_2-DCR) data integration in the water column and JO_2 based on Ba_{xs} content (Dehairs's transfer function; later referred to as JO_2-Ba). Similarly, to estimate JO_2-Ba in the present study we used the following equation [Dehairs et al., 1997] (Figure 3c):

$$JO_2\text{-Ba} = (Ba_{xs} - \text{Ba BKG})/17450 \quad (1)$$

A Ba BKG value of 130 pM was used (see above). JO_2-Ba is confronted to JO_2-Opt integrated over the same layer depth (between 175 and 450 m; Figure 3b). JO_2 rates are of the same order of magnitude (JO_2-Ba= 4.59 mmol m^{-2} d^{-1} and JO_2-opt= 3.14 mmol m^{-2} d^{-1}). The slight difference could be explained by the integration time of both methods: few hours to days for the incubations vs. few days to weeks for Ba_{xs} (seasonal build-up; Jacquet et al., 2007). JO_2 rates calculated in the present work are 3 times higher than those reported in the Southern Ocean during KEOPS1 [Jacquet et al., 2015] but they are in good agreement with the Ba_{xs} vs JO_2 trend (Figure 3b). DWA Ba_{xs} and JO_2 measured during KEOPS1 [Jacquet et al., 2015] and at ANTARES site (this study) are compared to Dehairs's relationship in Figure 3c. The correlation obtained in Lemaitre et al. [2018] in the North Atlantic is also reported (JO_2 were calculated from apparent oxygen utilisation divided by water mass age). Note that this relationship is not significantly different from the Dehairs's equation [Lemaitre et al., 2018]. Overall, results at the ANTARES site are lying along the Southern Ocean Ba_{xs} - JO_2 correlation. This further supports the validity of the Dehairs's transfer function in the present study.

3.4 Estimated particles remineralisation rates and implications

In order to provide a Ba_{xs}-derived estimate of POC remineralization rate (MR) at the ANTARES / EMSO-LO observatory during BATMAN cruise, we converted JO_2-Ba into C

respired using the Redfield (RR) C/O_2 molar ratio (127/175; Broecker et al., 1985) multiplied by the depth layer considered (Z, 175-450 m) [Dehairs et al., 1997]:

$$MR = Z \times JO_2\text{-}Ba \times RR \quad (2)$$

We obtain a POC remineralization rate of 11 mmol C m^{-2} d^{-1} (10% RSD). This is within the range of dissolved Ba- derived fluxes of POC remineralization (13 to 29 mmol C m^{-2} d^{-1}) reported in the Mediterranean Sea previously [Jacquet et al., 2016; Jullion et al., 2017]. Following calculations reported in Jullion et al. [2007], our MR rate would correspond to a Ba_{xs} flux of around 0.01 µmol m^{-2} d^{-1}. This is in reasonable agreement with barium fluxes (0.01 to 0.08 µmol m^{-2} d^{-1}) presented in Jullion et al. [2007]. Previously published barium fluxes from sediment trap range from 0.27 to 0.36 µmol m^{-2} d^{-1} at the DYFAMED station [Sternberg et al., 2007] and from 0.39 to 1.07 µmol m^{-2} d^{-1} in the Alboran Sea [Sanchez-Vidal et al., 2005]. POC remineralization rate from the present study is in the range of previously published carbon export fluxes (few to tens mmol m^{-2} d^{-1}) from thorium-derived data [Speicher et al., 2006] or from combining drifting sediment traps and underwater vision profilers [Ramondenc et al., 2016]. Constraining POC flux attenuation and remineralization rates in the Mediterranean is far from being achieved, especially regarding seasonal changes and inter-basin variations, but the concordance of the different approaches is promising.

4. CONCLUSIONS

The present paper brings a first insight into the connections of Ba_{xs}, PHP and JO_2 at the ANTARES/EMSO-LO observatory site in the northwestern Mediterranean Sea during the BATMAN (2016) cruise. Our results reveal a strong relationship between Ba_{xs} contents and measured JO_2 rates. Also, DWA Ba_{xs} vs. column integrated PHP, as well as measured vs. Ba_{xs}-based JO_2 relationships follow trends previously reported in the Southern Ocean where the

Dehairs's function was first established to estimate POC remineralisation rate. Results from the present study would indicate that this function can also be applied in the Mediterranean basin provided that adequate Ba_{xs} background values are estimated. From a global climate perspective, the Ba_{xs} tool will help to better balance the MedSea water column C budget. It will contribute to gain focus on the emerging picture of the C transfer efficiency (strength of the biological pump).

DATA AVAILABILITY

All data and metadata will be made available at the French INSU/CNRS LEFE CYBER database (scientific coordinator: Hervé Claustre; data manager, webmaster: Catherine Schmechtig). INSU/CNRSLEFE CYBER (2020)

AUTHOR CONTRIBUTION

SJ and DL designed the experiment for JO_2. SJ, CT and MG designed the experiments for PHP measurements. SJ and FLM managed barium sampling during the cruise. NB managed CTD deployment at sea. MG, SG and MR managed PHP. All co-authors contributed to writing.

COMPETING INTERESTS

The authors declare that they have no known competing financial interests or personal relationships that could have appeared to influence the work reported in this paper.

ACKNOWLEDGEMENTS

We thank the officers and crew of *R/V* EUROPE for their assistance during work at sea. This research was supported by the French national LEFE/INSU "REPAP" project (PI. S. Jacquet). It was co-funded by the "ROBIN" project (PIs. C. Tamburini, F.A.C. Le Moigne) of Labex OT-Med (ANR-11-LABEX-0061) funded by the Investissements d'Avenir and the French Government project of the ANR, through the A*Midex project (ANR-11-IDEX-0001-02). Authors have benefited of the support of the SNO-MOOSE and SAM-MIO. BATMAN is a

301 contribution to the "AT – POMPE BIOLOGIQUE" of the Mediterranean Institute of
302 Oceanography (MIO) and to the international IMBER program. The instrument (ELEMENT XR,
303 ThermoFisher) was supported in 2012 by European Regional Development Fund (ERDF).
304

Figure captions

Figure 1: (a) Schematic representation of the convergence of the different estimators of oxygen consumption and C remineralization rates from the "oxygen dynamics", "barium proxy" and "prokaryotic activity" tools; (b) Location of the BATMAN cruise at the ANTARES observatory site in the NW-Mediterranean Sea (42°48'N, 6°10'E). The location of the DYFAMED station is reported for comparison (Sternberg et al., 2008); (c) Potential temperature - salinity - depth plots and isopycals for BATMAN profiles. SW : Surface Water, WIW : Winter Intermediate Water, LIW : Levantine Intermediate Water, DMW : Deep Mediterranean Water. Graph constructed using Ocean Data View (Schlitzer, 2002; Ocean Data View; http://www.awi-bremerhaven.de/GEO/ODV)

Figure 2: (a) Particulate biogenic Ba_{xs} (pM) and particulate Al (nM) profiles next to the biogenic Ba fraction (%) in the upper 1000 m at ANTARES. The grey area represents a biogenic Ba fraction larger than 80 %. BKG: Ba_{xs} background. Ba_{xs} profile (pM) at DYFAMED : data from Sternberg et al. (2008); (b) ANTARES ratio plot (green square) of integrated PHP in the upper 100 m over integrated PHP in the upper 500 m versus depth-weighted average (DWA) mesopelagic Ba_{xs} (pM) over the 100-500m depth interval. Regression of the same ratio is reported for KEOPS1 (light blue symbols; out plateau stations) and KEOPS2 (dark blue symbols; Southern Ocean, Jacquet et al., 2015) and #DY032 (red square; PAP station, NE-Atlantic; pers. data) cruises. The blue line represents the trend obtained during KEOPS2 (Jacquet et al., 2015).

Figure 3: (a) Relationship between Ba_{xs} concentrations (pM) and oxygen consumption rates (µmol L^{-1} d^{-1}) from optodes measurements (JO_2-Opt) at ANTARES; (b) Confrontation of oxygen consumption rates (JO_2; mmol m^{-2} d^{-1}) obtained from different methods: optodes measurements

329 (this study; green square) and dark community respiration DCR (winkler titration; red triangles;
330 JO_2-DCR; Jacquet et al., 2015; KEOPS1), and Dehairs's transfer function calculation (Dehairs et
331 al., 1997) based on Ba_{xs} contents. The black line corresponds to the correlation obtained during
332 KEOPS1 (Jacquet et al., 2015); (c) Dehairs's relationship between depth-weighted average
333 (DWA) mesopelagic Ba_{xs} (pM) and JO_2 (µmol L^{-1} d^{-1}) compared to ANTARES result (this
334 study), KEOPS1 data (Southern Ocean; Jacquet et al., 2015) and GEOVIDE correlation (North
335 Atlantic; Lemaitre et al., 2018).
336

References

Bertram, Miriam, and James P. Cowen. "Morphological and Compositional Evidence for Biotic Precipitation of Marine Barite." *Journal of Marine Research* 55 (1997): 577–93.

Broecker, Wallace S. "'NO', a Conservative Water-Mass Tracer." *Earth and Planetary Science Letters* 23, no. 1 (August 1974): 100–107. doi:10.1016/0012-821X(74)90036-3.

Buesseler, Ken O., and Philip W. Boyd. "Shedding Light on Processes That Control Particle Export and Flux Attenuation in the Twilight Zone of the Open Ocean." *Limnology and Oceanography* 54, no. 4 (2009): 1210–32. doi:10.4319/lo.2009.54.4.1210.

Cardinal, Damien, Frank Dehairs, Thierry Cattaldo, and Luc André. "Geochemistry of Suspended Particles in the Subantarctic and Polar Frontal Zones South of Australia: Constraints on Export and Advection Processes." *Journal of Geophysical Research: Oceans* 106, no. C12 (décembre 2001): 31637–56. doi:10.1029/2000JC000251.

Cardinal D., Savoye N., Trull T. W., André L., Kopczynska E. E., and Dehairs F.: Variations of carbon remineralisation in the Southern Ocean illustrated by the Baxs proxy, Deep-Sea Res. Pt. I, 52, 355–370, https://doi.org/10.1016/j.dsr.2004.10.002, 2005.

Dehairs, F., R. Chesselet, and J. Jedwab. "Discrete Suspended Particles of Barite and the Barium Cycle in the Open Ocean." *Earth and Planetary Science Letters* 49, no. 2 (September 1980): 528–50. doi:10.1016/0012-821X(80)90094-1.

Dehairs, F., S. Jacquet, N. Savoye, B. A. S. Van Mooy, K. O. Buesseler, J. K. B. Bishop, C. H. Lamborg, et al. "Barium in Twilight Zone Suspended Matter as a Potential Proxy for

Particulate Organic Carbon Remineralization: Results for the North Pacific." *Deep Sea Research Part II: Topical Studies in Oceanography*, Understanding the Ocean's Biological Pump:results from VERTIGO, 55, no. 14–15 (juillet 2008): 1673–83. doi:10.1016/j.dsr2.2008.04.020.

Dehairs, F., C. E. Lambert, R. Chesselet, and N. Risler. "The Biological Production of Marine Suspended Barite and the Barium Cycle in the Western Mediterranean Sea." *Biogeochemistry* 4, no. 2 (June 1, 1987): 119–40. doi:10.1007/BF02180151.

Dehairs, F., D. Shopova, S. Ober, C. Veth, and L. Goeyens. "Particulate Barium Stocks and Oxygen Consumption in the Southern Ocean Mesopelagic Water Column during Spring and Early Summer: Relationship with Export Production." *Deep Sea Research Part II: Topical Studies in Oceanography* 44, no. 1–2 (1997): 497–516. doi:10.1016/S0967-0645(96)00072-0.

Ellison, Eurachem/CITAC Guide CG4, Quantifying Uncertainty in Analytical Measurement. Eds. S.L.R. Ellison, M. Rosslein and A. Williams. Second edition ISBN 0948926 15 5, Pp 120, 2000.

Giering, Sarah L. C., Richard Sanders, Richard S. Lampitt, Thomas R. Anderson, Christian Tamburini, Mehdi Boutrif, Mikhail V. Zubkov, et al. "Reconciliation of the Carbon Budget in the Ocean/'s Twilight Zone." *Nature* 507, no. 7493 (March 27, 2014): 480–83.

Hainbucher, D., A. Rubino, V. Cardin, T. Tanhua, K. Schroeder, and M. Bensi. "Hydrographic Situation during Cruise M84/3 and P414 (spring 2011) in the Mediterranean Sea." *Ocean Sci.* 10, no. 4 (juillet 2014): 669–82. doi:10.5194/os-10-669-2014.

Henson, Stephanie A., Richard Sanders, Esben Madsen, Paul J. Morris, Frédéric Le Moigne, and Graham D. Quartly. "A Reduced Estimate of the Strength of the Ocean's Biological Carbon Pump." *Geophysical Research Letters* 38, no. 4 (février 2011): L04606. doi:10.1029/2011GL046735.

IPCC Working Group 1, 5th Assessment Report (AR5) Climate Change 2013, Published in Jan. 2014.

Jacquet S.H.M., Dehairs F., Dumont I., Becquevort S., Cavagna A.-J., Cardinal, D.: Twilight zone organic carbon remineralization in the Polar Front Zone and Subantarctic Zone south of Tasmania, Deep-Sea Res. Pt. II, 58, 2222–2234, https://doi.org/10.1016/j.dsr2.2011.05.029, **2011**.

Jacquet, S. H. M., F. Dehairs, D. Lefèvre, A. J. Cavagna, F. Planchon, U. Christaki, L. Monin, L. André, I. Closset, and D. Cardinal. "Early Spring Mesopelagic Carbon Remineralization and Transfer Efficiency in the Naturally Iron-Fertilized Kerguelen Area." *Biogeosciences* 12, no. 6 (March 17, 2015): 1713–31. doi:10.5194/bg-12-1713-2015.

Jacquet, S. H. M., F. Dehairs, N. Savoye, I. Obernosterer, U. Christaki, C. Monnin, and D. Cardinal. "Mesopelagic Organic Carbon Remineralization in the Kerguelen Plateau Region Tracked by Biogenic Particulate Ba." *Deep Sea Research Part II: Topical Studies in Oceanography*, KEOPS: Kerguelen Ocean and Plateau compared Study, 55, no. 5–7 (March 2008): 868–79. doi:10.1016/j.dsr2.2007.12.038, 2008b

Jacquet, S. H. M., J. Henjes, F. Dehairs, A. Worobiec, N. Savoye, and D. Cardinal. "Particulate Ba-Barite and Acantharians in the Southern Ocean during the European Iron Fertilization

399 Experiment (EIFEX).” *Journal of Geophysical Research* 112, no. G4 (October 23, 2007).
400 doi:10.1029/2006JG000394.

401 Jacquet, S.H.M., C. Monnin, V. Riou, L. Jullion, and T. Tanhua. “A High Resolution and Quasi-
402 Zonal Transect of Dissolved Ba in the Mediterranean Sea.” *Marine Chemistry* 178 (January
403 20, 2016): 1–7. doi:10.1016/j.marchem.2015.12.001.

404 **Jacquet** S.H.M., Savoye N., Dehairs F., Strass V.H., Cardinal D.: Mesopelagic carbon remineralization
405 during the European Iron Fertilization Experiment, Global Biogeochem. Cy., 22, 1–9,
406 https://doi.org/10.1029/2006GB002902, **2008a**.

407 Jullion, L., S. H. M. Jacquet, and T. Tanhua. “Untangling Biogeochemical Processes from the
408 Impact of Ocean Circulation: First Insight on the Mediterranean Dissolved Barium
409 Dynamics.” *Global Biogeochemical Cycles* 31, no. 8 (2017): 1256–70.
410 doi:10.1002/2016GB005489.

411 Kirchman DL (1993) Leucine incorporation as a measure of biomass production by heterotrophic
412 bacteria. In: Kemp PF, Sherr BF, Sherr EB, Cole JJ (eds) Handbooks of methods in aquatic
413 microbial ecology. Lewis Publishers, Boca Raton, Ann Arbor, London, Tokyo, p 509–512

414 Lemaitre, N., H. Planquette, F. Planchon, G. Sarthou, S. Jacquet, M. I. García-Ibáñez, A.
415 Gourain, et al. “Particulate Barium Tracing of Significant Mesopelagic Carbon
416 Remineralisation in the North Atlantic.” *Biogeosciences* 15, no. 8 (2018): 2289–2307.
417 doi:10.5194/bg-15-2289-2018.

418 Malanotte-Rizzoli, P., V. Artale, G. L. Borzelli-Eusebi, S. Brenner, A. Crise, M. Gacic, N. Kress,
419 et al. “Physical Forcing and Physical/biochemical Variability of the Mediterranean Sea: A

Review of Unresolved Issues and Directions for Future Research." *Ocean Science* 10, no. 3 (2014): 281–322. doi:10.5194/os-10-281-2014.

Martin, John H., George A. Knauer, David M. Karl, and William W. Broenkow. "VERTEX: Carbon Cycling in the Northeast Pacific." *Deep Sea Research Part A. Oceanographic Research Papers* 34, no. 2 (1987): 267–85. doi:http://dx.doi.org/10.1016/0198-0149(87)90086-0.

Martinez-Ruiz, Francisca, Fadwa Jroundi, Adina Paytan, Isabel Guerra-Tschuschke, María del Mar Abad, and María Teresa González-Muñoz. "Barium Bioaccumulation by Bacterial Biofilms and Implications for Ba Cycling and Use of Ba Proxies." *Nature Communications* 9, no. 1 (April 24, 2018): 1619. doi:10.1038/s41467-018-04069-z.

Martinez-Ruiz, F., A. Paytan, M.T. Gonzalez-Muñoz, F. Jroundi, M.M. Abad, P.J. Lam, J.K.B. Bishop, T.J. Horner, P.L. Morton, and M. Kastner. "Barite Formation in the Ocean: Origin of Amorphous and Crystalline Precipitates." *Chemical Geology* 511 (April 20, 2019): 441–51. doi:10.1016/j.chemgeo.2018.09.011.

Ramondenc, Simon, Goutx Madeleine, Fabien Lombard, Chiara Santinelli, Lars Stemmann, Gabriel Gorsky, and Lionel Guidi. "An Initial Carbon Export Assessment in the Mediterranean Sea Based on Drifting Sediment Traps and the Underwater Vision Profiler Data Sets." *Deep Sea Research Part I: Oceanographic Research Papers* 117 (November 2016): 107–19. doi:10.1016/j.dsr.2016.08.015.

439 Sanchez-Vidal, A., R. W. Collier, A. Calafat, J. Fabres, and M. Canals (2005), Particulate barium
440 fluxes on the continental margin: A study from the Alboran Sea (Western Mediterranean),
441 Mar. Chem., 93, 105–117.

442 Santinelli, Chiara, Luciano Nannicini, and Alfredo Seritti. "DOC Dynamics in the Meso and Bathypelagic
443 Layers of the Mediterranean Sea." *Deep Sea Research Part II: Topical Studies in Oceanography*,
444 Ecological and Biogeochemical Interactions in the Dark Ocean, 57, no. 16 (août 2010): 1446–59.
445 doi:10.1016/j.dsr2.2010.02.014.

446 Siegel DA, Buesseler KO, Behrenfeld MJ, Benitez-Nelson CR, Boss E, Brzezinski MA, Burd A, Carlson
447 CA, D'Asaro EA, Doney SC, Perry MJ, Stanley RHR and Steinberg DK (2016) Prediction of the
448 Export and Fate of Global Ocean Net Primary Production: The EXPORTS Science Plan. *Front. Mar.*
449 *Sci*. 3:22. doi: 10.3389/fmars.2016.00022

450 Simon M, Azam F (1989) Protein content and protein synthesis rates of planktonic marine
451 bacteria. Mar Ecol Prog Ser 51:201–213

452 Shopova, D., F. Dehairs, and W. Baeyens. "A Simple Model of Biogeochemical Element
453 Distribution in the Oceanic Water Column." *Journal of Marine Systems* 6, no. 4 (juin 1995):
454 331–44. doi:10.1016/0924-7963(94)00032-7.

455 Speicher, E. A., S. B. Moran, A. B. Burd, R. Delfanti, H. Kaberi, R. P. Kelly, C. Papucci, et al.
456 "Particulate Organic Carbon Export Fluxes and Size-Fractionated POC/234Th Ratios in the
457 Ligurian, Tyrrhenian and Aegean Seas." *Deep Sea Research Part I: Oceanographic*
458 *Research Papers* 53, no. 11 (2006): 1810–30.
459 doi:http://dx.doi.org/10.1016/j.dsr.2006.08.005.

460 Sternberg, E., C. Jeandel, E. Robin, and M. Souhaut. “Seasonal Cycle of Suspended Barite in the
461 Mediterranean Sea.” *Geochimica et Cosmochimica Acta* 72, no. 16 (2008): 4020–34.
462 doi:https://doi.org/10.1016/j.gca.2008.05.043.

463 Tamburini C, Canals M, Durieu de Madron X, Houpert L, Lefèvre D, Martini S, D’Ortenzio F,
464 Robert A, Testor P, and the ANTARES collaboration (2013) Deep-sea bioluminescence
465 blooms after dense water formation at the ocean surface. PLoS One 8:e67523

466 Tamburini C, Garcin J, Ragot M, Bianchi A (2002) Biopolymer hydrolysis and bacterial
467 production under ambient hydrostatic pressure through a 2000 m water column in the NW
468 Mediterranean. Deep Res II 49:2109–2123

469 Taylor, S.R., McLennan, S.M.: The continental crust: its composition and evolution, Blackwell
470 Scientific Publications, 312pp, 1985.

471

472

473

474

475

476

477

478

479

480 FIGURE 1

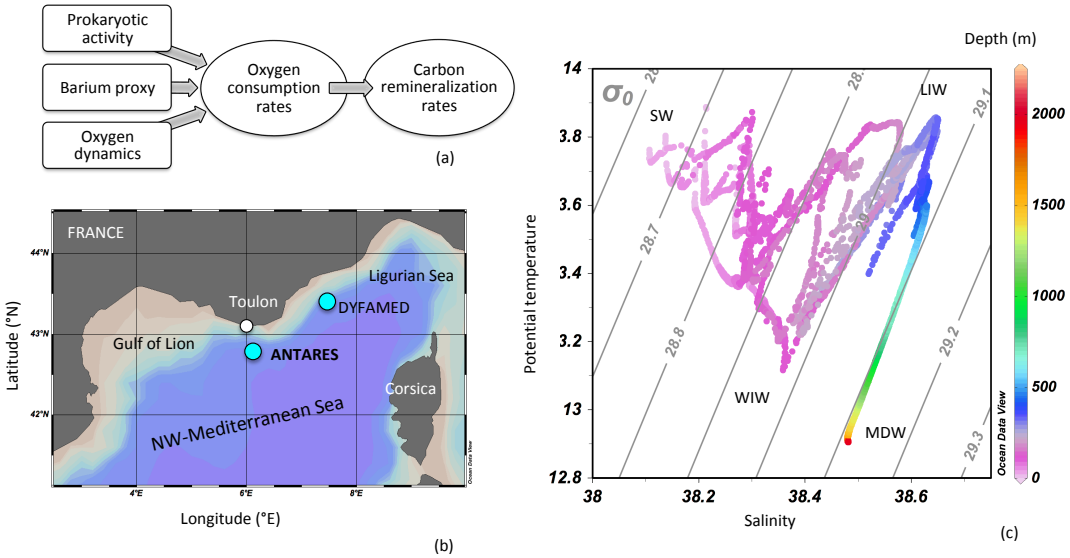

481

482 FIGURE 2

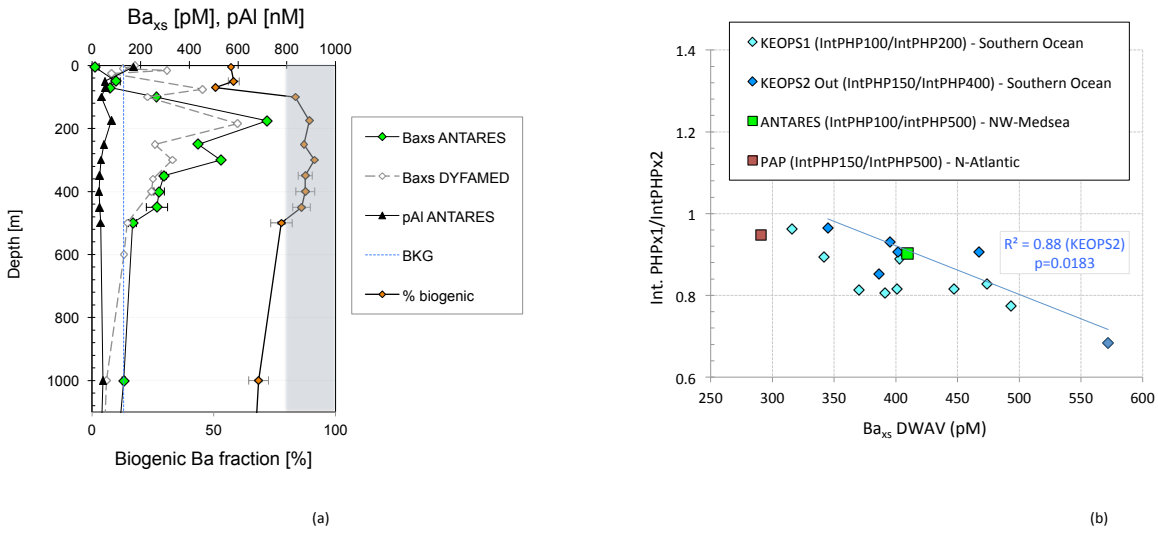

483

484

485

FIGURE 3

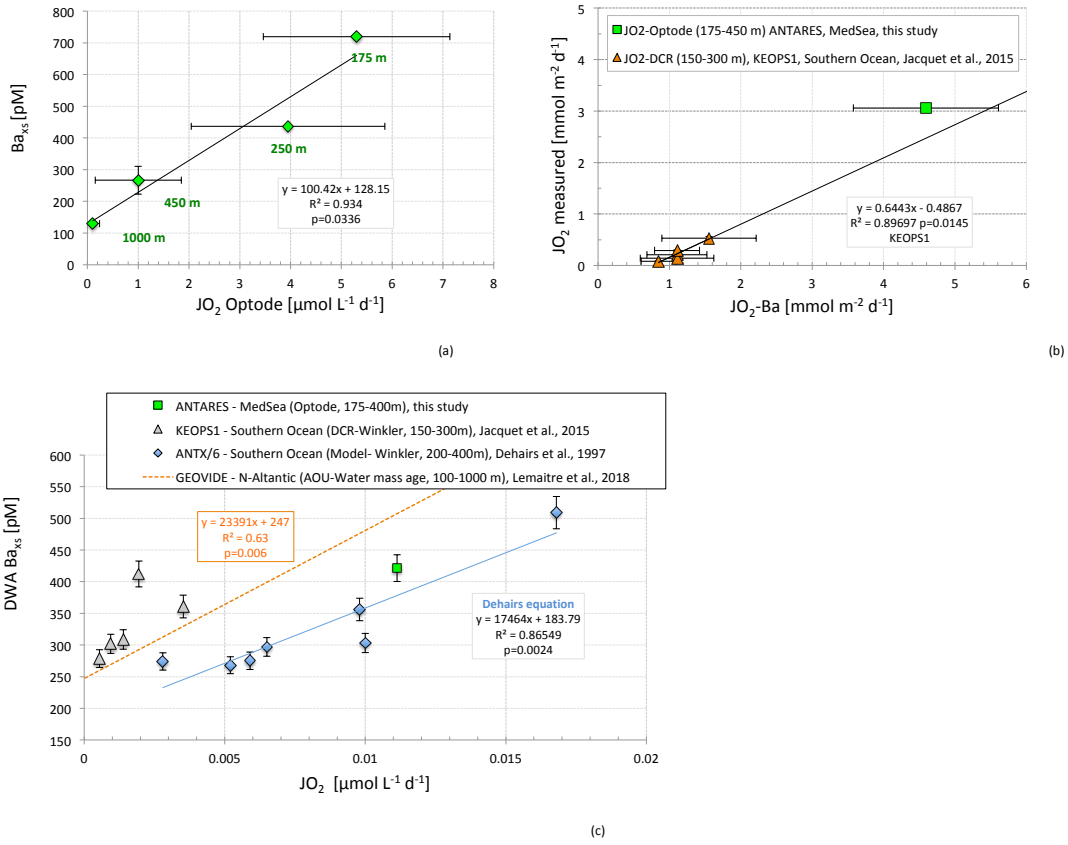
Ba$_{xs}$ [pM]
JO$_2$ Optode [µmol L^{-1} d^{-1}]
175 m
250 m
450 m
1000 m
y = 100.42x + 128.15
R² = 0.934
p=0.0336
(a)
JO2-Optode (175-450 m) ANTARES, MedSea, this study
JO2-DCR (150-300 m), KEOPS1, Southern Ocean, Jacquet et al., 2015
JO$_2$ measured [mmol m^{-2} d^{-1}]
JO$_2$-Ba [mmol m^{-2} d^{-1}]
y = 0.6443x - 0.4867
R² = 0.89697 p=0.0145
KEOPS1
(b)
ANTARES - MedSea (Optode, 175-400m), this study
KEOPS1 - Southern Ocean (DCR-Winkler, 150-300m), Jacquet et al., 2015
ANTX/6 - Southern Ocean (Model- Winkler, 200-400m), Dehairs et al., 1997
GEOVIDE - N-Altantic (AOU-Water mass age, 100-1000 m), Lemaitre et al., 2018
DWA Ba$_{xs}$ [pM]
y = 23391x + 247
R² = 0.63
p=0.006
Dehairs equation
y = 17464x + 183.79
R² = 0.86549
p=0.0024
JO$_2$ [µmol L^{-1} d^{-1}]
(c)